JPSE (Journal of Physical Science and Engineering), Vol. 7, No. 2, 2022, Page 99–107.
DOI: 10.17977/um024v7i22022p099

JPSE
(Journal of Physical Science and Engineering)

http://journal2.um.ac.id/index.php/jpse
EISSN: 2541-2485

Implementation of Line of Sight Algorithm Design Using Quadcopter on Square Tracking

Received
10 September 2021

Revised
12 September 2022

Accepted for Publication
09 October 2022

Published
30 December 2022

A T Nugraha[1], D Rinaldi[1], M S Messiah[2], M J Shiddiq[2], M F Ramadhan[2], and F H Ainudin[1]

[1.] Department of Marine Electrical Engineering, Faculty of Shipbuilding Electrical Engineering, Shipbuilding Institute of Polytechnic Surabaya, Jl. Teknik Kimia Keputih Sukolilo, Surabaya, 60111, Indonesia.
[2.] Department of Automation Engineering, Faculty of Shipbuilding Electrical Engineering, Shipbuilding Institute of Polytechnic Surabaya, Jl. Teknik Kimia Keputih Sukolilo, Surabaya, 60111, Indonesia.

***E-mail:** anggaranugraha@ppns.ac.id

Abstract
The improvement of the quadcopter has extended its function, even for risky army tasks, i.e., search, reconnaissance, and rescue operations. The quadcopter also can be implemented for medical tasks, such as mapping wind velocity conditions, detecting radiation sources, surveillance, and upkeep and surveys. A quadcopter is a non-linear machine with more than one enter and output and a machine with balance problems. It is simply prone to outside disturbance. This function reasons a few problems in controlling the monitoring motion and adjusting the dealing with the path automatically. Based on those problems, this looks like the monitoring manipulated layout within the horizontal place with the aid of including the line of sight's set of rules. So, that direction following converges closer to 0 and may conquer the disturbance of ocean currents that extrude the parameters of the quadcopter in shifting at the horizontal place. The controller benefit is acquired using the numerical iterative of the Linear Matrix Inequality (LMI) technique. Meanwhile, Command-Generator Tracker (CGT) controls the monitoring function at the x and y. The simulation effects display that the manipulation technique can deliver the yaw, pitch, and roll to the anticipated values on a rectangular track.
Keywords: Quadcopter UAV, square track, LMI, CGT, LQ regulator.

1. Introduction

Several trends are persevering to be accomplished to enhance the reaction of the quadcopter machine in monitoring the issues that occur [1]. It performs rectangular monitoring using the highest quality technique, named highest quality output comments, by including a shape from the Command-Generator Tracker (CGT), which is used to get a signal of monitoring reference according to the hint blunders as small as possible. The output comments controller has *H* overall performance to preserve its stability, so the quadcopter is extra dependable in dealing with disturbances [2].

Nonstop improvement techniques are used to address the management issues at the quadcopter, in which nonlinear strategies are used for hover management [3]. Meanwhile, the back-stepping technique is extra appropriate for nonlinear machines [4]. So, the stairs calculation used in its technique may need to be simplified. Even with its complication [5], the quadcopter can follow the direction in step with the references of the situations from the x, y, and z values [6]. However, while the quadcopter is disturbed through the shape of the regular wind, its reaction is ripple and now no longer robust. In [7], the Line Of Sight (LOS) set of rules is offered, which makes it clean to regulate the route of a plant in order that it converges to a described direction by making the supposed cross-song blunders [8].

Based on the issues and answers above, the concept within the examination will be proposed to lay out the highest quality management technique to manage the quadcopter [9], so it could follow a predetermined direction. Additionally, it could upload the LOS set of rules that have been used to produce conformity to a direction shape as a reference sign by putting the route of the face and the direction blunders as small as possible [10], [11].

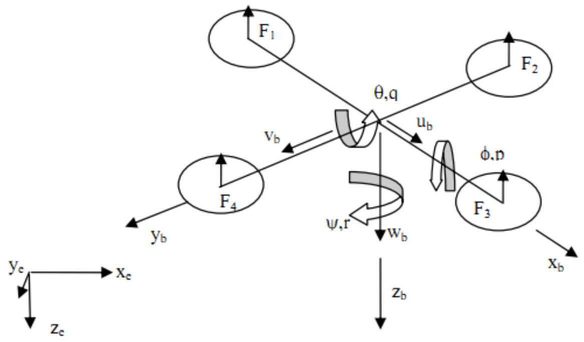

Figure 1. Quadcopter's states (e = earth frame, b = body frame).

The concept states that it will additionally lay out the highest quality management technique to manipulate the quadcopter in a rectangular song [12]. Output comments manage *H∞* overall performance to preserve stability [13]. The direction-following controller uses the CGT with the subsequent version and provides the LOS set of rules used to generate conformity to the direction form as a reference sign by putting the route and blunders of the present direction as small as possible [14].

2. Method

2.1. Quadcopter Design

The physical layout is complicated without suppositions used to simplify the equation on the quadcopter, as shown in Figure 1. Twelve outputs of six DoF (Degrees of Freedom) exist on this quadcopter. Six of twelve outputs will determine the quadcopter's attitude [15], [16]. Its kinematic and dynamic layout are derived primarily based totally on Newton-Euler with numerous simplifying assumptions [17], such as the shape is thought to be inflexible or symmetrical, the propeller is thought to be inflexible, and others.

Thrust and drag are cheap with a couple of paces from the propeller. The translational axis lies on the earth's coordinates need to change from the body frame into the earth's frame [18]. So, a transition matrix is needed ${}_{B}^{E}R$ (Equation 1), which gains from the multiplication of x, y, and z.

$$ {}_{B}^{E}R = \begin{bmatrix} c\theta c\psi & -c\varphi s\psi + s\varphi s\theta s\psi & s\varphi s\psi \\ c\theta s\psi & c\varphi c\psi + s\varphi s\theta s\psi & -s\varphi c\psi + c\varphi s\theta s\psi \\ -s\theta & s\varphi c\theta & c\varphi c\theta \end{bmatrix} \tag{1} $$

To simplify, we use s as sin and c as cos.

2.2. Dynamic Linearization Design

This section will explain approximately the dynamic linearization, which the dynamic idea is already defined withinside section 2.1. The equation might be linearized while the quadcopter is in a soaring condition. The yaw angle is 0 rad, and the angular velocity of roll, pitch, and yaw is close to 0 rad/s [20], [21]. Variable state v will be used as a dynamic representation of the quadcopter actuator, as shown in Equation 2.

$$ v = \frac{\omega}{s+\omega} u \tag{2} $$

This parameter is used as a reference for controller arrangement and simulation. For example, the rotation around x and y is decoupled, there is a motion in the roll/pitch. If the drag constant is ignored, the quadcopter will be considered in a hovering state when approaching the acceleration of the quadcopter.

$$ \begin{gathered} \varphi << 0.1 \Rightarrow \sin(\varphi) \cong 0, \cos(\varphi) \cong 1 \\ \theta << 0.1 \Rightarrow \sin(\theta) \cong 0, \cos(\theta) \cong 1 \end{gathered} \tag{3} $$

The assumed roll/pitch θ can be formulated using Equation 4,

$$ J\ddot{\theta} = \Delta F l \tag{4} $$

with $J = J_{\text{roll}} = J_{\text{pitch}}$, l is the propeller distance from the gravity center, and $\Delta F = F_1 - F_2$. There is a difference between the forces produced by the two machines. The difference in the forces generated by the different inputs for the two machines is $\Delta u = u_1 - u_2$.

The state space for the linear model of roll and pitch dynamics can be expressed in Equations 5 and 6,

$$\begin{bmatrix} \dot{\varphi} \\ \ddot{\varphi} \\ \dot{v} \end{bmatrix} = \begin{bmatrix} 0 & 1 & 0 \\ 0 & 0 & \dfrac{lK_T}{J} \\ 1 & 0 & -\omega \end{bmatrix} \begin{bmatrix} \varphi \\ \dot{\varphi} \\ v \end{bmatrix} + \begin{bmatrix} 0 \\ 0 \\ \omega \end{bmatrix} \Delta u_2 \tag{5}$$

$$\begin{bmatrix} \dot{\theta} \\ \ddot{\theta} \\ \dot{v} \end{bmatrix} = \begin{bmatrix} 0 & 1 & 0 \\ 0 & 0 & \dfrac{lK_T}{J} \\ 1 & 0 & -\omega \end{bmatrix} \begin{bmatrix} \theta \\ \dot{\theta} \\ v \end{bmatrix} + \begin{bmatrix} 0 \\ 0 \\ \omega \end{bmatrix} \Delta u_1 \tag{6}$$

The linear dynamics design which generated in the x and y in the state space as shown in Equations 7 and 8,

$$\begin{bmatrix} \dot{x} \\ \ddot{x} \\ \dot{v} \end{bmatrix} = \begin{bmatrix} 0 & 1 & 0 \\ 0 & 0 & \dfrac{4K_T}{J}\theta \\ 0 & 0 & -\omega \end{bmatrix} \begin{bmatrix} x \\ \dot{x} \\ v \end{bmatrix} + \begin{bmatrix} 0 \\ 0 \\ \omega \end{bmatrix} u \tag{7}$$

$$\begin{bmatrix} \dot{y} \\ \ddot{y} \\ \dot{v} \end{bmatrix} = \begin{bmatrix} 0 & 1 & 0 \\ 0 & 0 & \dfrac{4K_T}{J}\varphi \\ 0 & 0 & -\omega \end{bmatrix} \begin{bmatrix} y \\ \dot{y} \\ v \end{bmatrix} + \begin{bmatrix} 0 \\ 0 \\ \omega \end{bmatrix} u \tag{8}$$

2.3. *Quadcopter's Block Diagram*

Figure 2 is a block diagram from the quadcopter's control strategy that will be designed. The control structure consists of inner and outer loops. The inner loop is a controller of the angle rotation (φ, θ, ψ), which adds an extra performance $H\infty$ (yellow fill), then the outer loop is a tracking controller (x, y, z), which uses the CGT (red fill) that contains the LOS algorithm. The reference signal controls the quadcopter's system and consists of the position x_d, y_d, z_d, and ψ_d angle.

The inner loop is used to stabilize roll, pitch, and yaw, which will ensure its performance. A controller can be designed based on the Static Output Feedback (SOF) problem [7]. The gain output feedback can be obtained by solving the iterative Linear Matrix Inequality (LMI) algorithm.

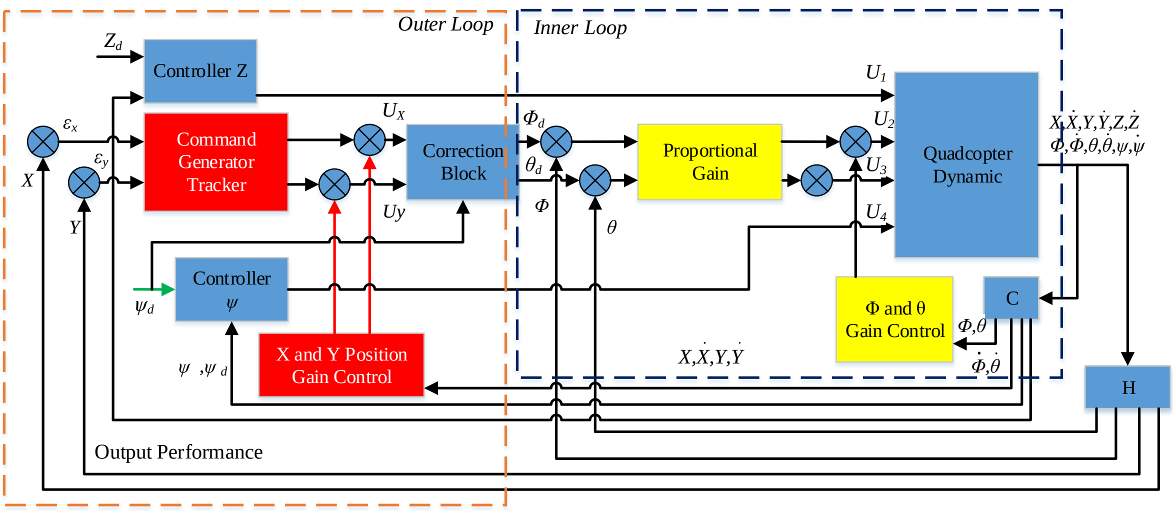

Figure 2. Quadcopter's block diagram.

2.4. Line Of Sight (LOS) Terms in the Steering Equation

Speed vector to the intersection point $\boldsymbol{P}_{\text{LOS}}^{n} = [x_{\text{LOS}}, y_{\text{LOS}}]^T$ to match the path with an enclosure-based strategy to drive $e(t)$ to zero, where the predefined waypoint sequence is an implicit path definition. The path directly involves determination by Equation 9.

$$\tan\big(\chi_d(t)\big) = \frac{\Delta y(t)}{\Delta x(t)} = \frac{y_{\text{LOS}} - y(t)}{x_{\text{LOS}} - x(t)} \tag{9}$$

The center coordinates of an engine $\{b\}$ is defined by $\boldsymbol{P}^n = [x, y]^T$ and used in a square with the radius $R > 0$, which is pulled out from the center point of the engine $\{b\}$. That square will cut a path in the two coordinates, which one is $(x_{\text{LOS}}, y_{\text{LOS}})$. The counting of the unknown two coordinates of LOS $\boldsymbol{P}_{\text{LOS}}^{n} = [x_{\text{LOS}}, y_{\text{LOS}}]^T$ can be solved by Equations 10 and 11.

$$[x_{\text{LOS}} - x(t)]^2 + [y_{\text{LOS}} - y(t)]^2 = R^2 \tag{10}$$

$$\tan(\alpha_k) = \frac{y_{k+1} - y_k}{x_{k+1} - x_k} = \frac{y_{\text{LOS}} - y_k}{x_{\text{LOS}} - x_k} = \text{constant} \tag{11}$$

It is a pythagoras, while the formula represents the slope angle from the path to the earth's axis as x α_k. The slope between the two waypoints is constant, and their amount is also valid. The calculation process of enclosure is analytically based on [3], with the first argument that $|\Delta x| > 0$, can be described by Equation 12,

$$y_{\text{LOS}} = \frac{\Delta y}{\Delta x}(x_{\text{LOS}} - x_k) + y_k \tag{12}$$

with $\Delta x \coloneqq x_{k+1} - x_k$ and $\Delta y \coloneqq y_{k+1} - y_k$ are the difference position x and y between two waypoints.

2.5. The Control System Design using Command-Generator Tracker (CGT)

The LMI's form that used the Schur Complement is

$$\begin{bmatrix} P_n A + A^T P_n + Q + L_n^T R^{-1} L_n & P_n B & P_n D \\ B^T P_n & R & 0 \\ D^T P_n & 0 & -\gamma^2 I \end{bmatrix} \leq 0 \tag{13}$$

The linearized system state for roll, pitch and yaw becomes

$$x_{\text{inner}} = [\varphi \quad p \quad v \quad \theta \quad q \quad v \quad \psi \quad r]^T \tag{14}$$

The main variables to be controlled are roll and pitch and the three speeds, namely roll, pitch, and yaw, when designing a rotation controller. So, the output vector of the controller is

$$y_{\text{inner}} = [\varphi \quad \theta \quad \psi \quad p \quad q]^T \tag{15}$$

If the roll and pitch are equal in the inertia ($J_{xx} = J_{yy} = 0.03$ kg.m^2), the roll and pitch dynamics are also same (Equation 16).

$$\begin{bmatrix} \dot{\varphi} \\ \ddot{\varphi} \\ \dot{v} \end{bmatrix} = \begin{bmatrix} 0 & 1 & 0 \\ 0 & 0 & 800 \\ 0 & 0 & -15 \end{bmatrix} \begin{bmatrix} \varphi \\ \dot{\varphi} \\ v \end{bmatrix} + \begin{bmatrix} 0 \\ 0 \\ 15 \end{bmatrix} \Delta u \tag{16}$$

The state space of roll/pitch linear shown in Equations 17 and 18.

$$y_\varphi = C_\varphi \begin{bmatrix} \varphi \\ \dot{\varphi} \\ v \end{bmatrix} = \begin{bmatrix} 1 & 0 & 0 \\ 0 & 0.1 & 0 \end{bmatrix} \begin{bmatrix} \varphi \\ \dot{\varphi} \\ v \end{bmatrix} \tag{17}$$

$$Z_\varphi = H x_\varphi = [0.7 \quad 0 \quad 0] \begin{bmatrix} \varphi \\ \dot{\varphi} \\ v \end{bmatrix} \tag{18}$$

From the parameter values, the best results are generated as $\gamma = 0.9$, $R = 15$, and $Q = \text{diag}\{775, 3, 0.1\}$.

By using the iterative LMI feasibility method, a matrix result in p and K after the twelfth iteration is

$$p=\begin{bmatrix}29.8331 & 0.1572 & 0.4897\\ 0.1572 & 0.0156 & 0.0545\\ 0.4897 & 0.0545 & -\gamma^2 I\end{bmatrix};K=[0.7461 \quad 0.0718] \tag{19}$$

The objective of position tracking control aims to create a quadcopter following the expected trajectory while the quadcopter is flying. In this manner, the given reference flag points to track the x position, which may be a sinusoidal flag with a recurrence of 0.1047 rad/s or break even with 0.0167 Hz with a stage of -0.26 rad. Here is the reference flag condition $x_d=-\sin(0.05\pi t)$. If it is changed using the Laplace transform, then the transfer function is $\Delta(p)x_d=p^2+0.02=0$, so

$$\dot{x}_d=\begin{bmatrix}0 & 1\\ -0.02 & 0\end{bmatrix}x_d=Gx_d \tag{20}$$

The augmented system is obtained from the quadcopter dynamics for x is

$$\begin{bmatrix}\dot{\varepsilon}\\ \ddot{\varepsilon}\\ \dot{x}\\ \ddot{x}\\ \dot{v}\end{bmatrix}=\begin{bmatrix}0 & 1 & 0 & 0 & 0\\ -0.02 & 0 & -1 & 0 & 0\\ 0 & 0 & 0 & 1 & 0\\ 0 & 0 & 0 & 0 & 136.2683\\ 0 & 0 & 0 & 0 & -15\end{bmatrix}\begin{bmatrix}\varepsilon\\ \dot{\varepsilon}\\ x\\ \dot{x}\\ v\end{bmatrix}+\begin{bmatrix}0\\ 0\\ 0\\ 0\\ 15\end{bmatrix}U_1 \tag{21}$$

with the output performance

$$\tilde{y}=\tilde{C}\tilde{x}=\begin{bmatrix}J & 0\\ 0 & C\end{bmatrix}\begin{bmatrix}\varepsilon\\ x\end{bmatrix}=\begin{bmatrix}1 & 0 & 0 & 0\\ 0 & 1 & 0 & 0\\ 0 & 0 & 1 & 0\\ 0 & 0 & 0 & 1\end{bmatrix}\begin{bmatrix}\varepsilon\\ \dot{\varepsilon}\\ x\\ \dot{x}\\ v\end{bmatrix} \tag{22}$$

The path that we want to provide as the reference signal for the quadcopter is a square form (in the three-dimensional area). Therefore, the reference signal given for the y position is

$$Y_d=-1-cos(0.05\pi t) \tag{23}$$

A similar characteristic of the polynomial is $\Delta(p)y_d=p^3+0.02p=0$. From the reference signal with the order d = 3 and then written in the form of a state space's matrix of 3 × 3 dimensions. The representation of the reference signal is the CGT structure. So, not all derivatives of the reference signal need to be used in the system structure, so modifications are made in this design and can be written as

$$\Delta(p)y_d=0.02p=0 \Rightarrow \dot{y}_d=\begin{bmatrix}0 & 1\\ 0 & -0.02\end{bmatrix}y_d=Gy_d \tag{24}$$

So, the modification of the multiple augmented system for the dynamic position at y is

$$\begin{bmatrix}\dot{\varepsilon}\\ \ddot{\varepsilon}\\ \dot{y}\\ \ddot{y}\\ \dot{v}\end{bmatrix}=\begin{bmatrix}0 & 1 & 0 & 0 & 0\\ 0 & -0.02 & -1 & 0 & 0\\ 0 & 0 & 0 & 1 & 0\\ 0 & 0 & 0 & 0 & -136.2683\\ 0 & 0 & 0 & 0 & -15\end{bmatrix}\begin{bmatrix}\varepsilon\\ \dot{\varepsilon}\\ y\\ \dot{y}\\ v\end{bmatrix}+\begin{bmatrix}0\\ 0\\ 0\\ 0\\ 15\end{bmatrix}U_1$$

$$\tilde{y}=\begin{bmatrix}1 & 0 & 0 & 0\\ 0 & 1 & 0 & 0\\ 0 & 0 & 1 & 0\\ 0 & 0 & 0 & 1\end{bmatrix}\begin{bmatrix}\varepsilon\\ \dot{\varepsilon}\\ y\\ \dot{y}\\ v\end{bmatrix} \tag{25}$$

The parameter value used for the simulation is in Table 1. Gain feedback output $\widetilde{K}$ which is used for the position controller x, y is generated by

$$\widetilde{K}_x=[-4.418 \quad -9.4 \quad 9{,}454 \quad 5.3433] \tag{26}$$

and

$$\widetilde{K}_y=[15.9326 \quad 23.31 \quad -15.8108 \quad -6.2181] \tag{27}$$

Table 1. The algorithm of the path following straigh line [3].

Path following Straigh Line (Straight Line) Algorithm With LOS
1. Waypoint initialisation until used by generate path $P_k^n = [x_k, y_k]^T$ and $P_{k+1}^n = [x_k, y_k]^T$
2. For every iteration error calculation between position with quadcopter actual position $p^n = [x(t), y(t)]^T$ and $P_k^n = [x_k, y_k]^T$
3. Specify LOS point through how many meters it is desired from the waypoint are $p_{los}^n = [x_{los}, y_{los}]^T$, $P_k^n = [x_k, y_k]^T$, and $P_{k+1}^n = [x_k, y_k]^T$
4. Calculate absolute *error* value between waypoint position with actual quadcopter $\lvert e_p \rvert = \sqrt{(x_{los} - x(t))^2 + (y_{los} - y(t))^2}$
5. Calculate ψ angle with $\psi_d = a\tan 2\,(x_{\mathrm{LOS}} - x(t), y_{\mathrm{LOS}} - y(t))$

3. Result and Discussion

Matlab is used to determine the following path quadcopter's effectiveness. The simulation is carried out to test the movement of the quadcopter and whether it can follow a path for a square trajectory as a reference for tracking its movement. Quanser Qb all-X4 is a type of quadcopter used in this simulation. Testing the movement of the quadcopter using simulation is done to determine whether the quadcopter can perform the following path for a square trajectory, as shown in Figure 3. The direction of the quadcopter used is the same as that of the quadcopter movement used in this simulation. Considering the quadcopter direction aims to make the quadcopter movement smoother and maintain its direction.

By adding the LOS algorithm, to calculate the headings, the yaw (ψ) can also be counted. By observing the yaw, the reference signal can be stored by the quadcopter from the outer loop output controller with an average cross-trajectory error of 0.0245 rad. From the comparison between actual yaw and reference yaw, it can be concluded that the heading is well maintained, which can be seen in Figure 4.

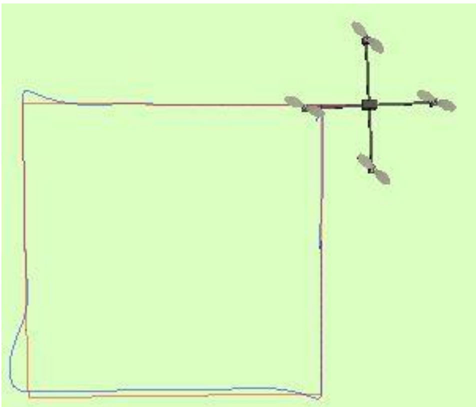

Figure 3. Quadcopter's movement on the *x* and *y* axis.

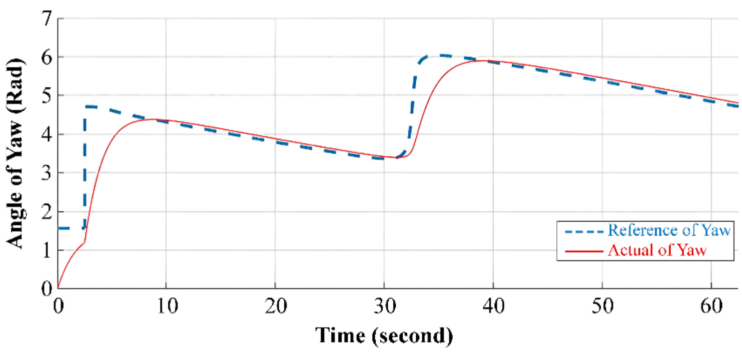

Figure 4. Quadcopter's path in yaw.

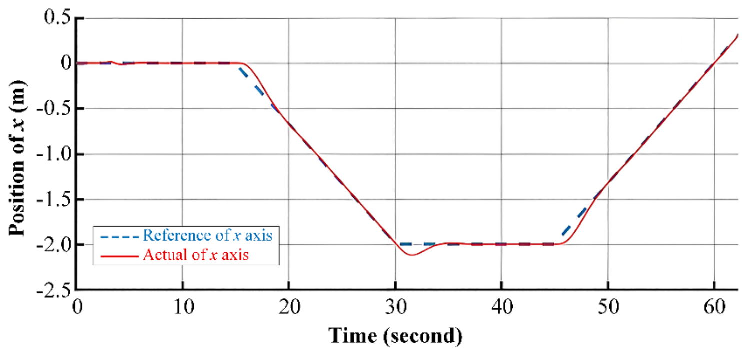

Figure 5. Quadcopter's path in *x* axis.

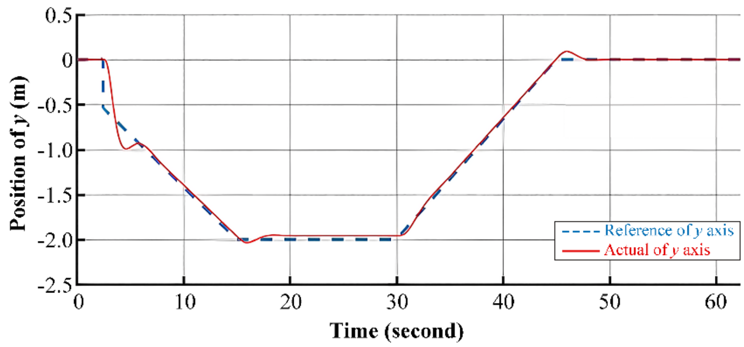

Figure 6. Quadcopter's path in *y* axis.

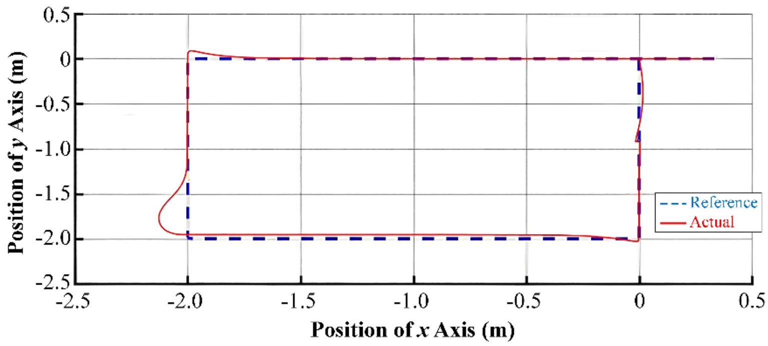

Figure 7. The difference between reference and actual tour in the square path.

The position of the quadcopter at x that can follow the reference can be seen in Figure 5. The following statement is the path at $t = 15$ seconds and a delay of about 2 seconds, which causes an error of 0.3 m, but the quadcopter can still track the reference path. The movement on the y axis, where the quadcopter has a delay of about 0.4 seconds at the first waypoint and causes an error path of about 0.3 m, but the quadcopter can return to the reference path, as shown in Figure 6. A squared reference signal is added to the system in Figure 7. The result is that the quadcopter continues to follow the path, but a deviation occurs at $x = 0.5$ m and $y = 0.2$ m. The LOS algorithm helps control the quadcopter by providing a smooth adjustment at 90°, and it still follows the reference.

4. Conclusion

The output manipulates comments with $H\infty$ overall performance used withinside the internal loop, while the CGT withinside the outer loop. The simulation consequences display that the manipulated gadget is capable of stabilizing the quadcopter's mindset attitude and tuning the reference sign given to itself. The highest rating of ISE monitoring is 0.1 m, while there may be no distraction, while 0.28 otherwise. The controller can make the quadcopter tracks itself with the rectangular and helix tune references.

References

[1] T. Luukkonen, (Aug. 2011). Modelling and control of quadcopter [Online]. Available: https://www.researchgate.net/file.PostFileLoader.html?id=576d16ed93553b24b5721a9a&assetKey=AS%3A376462596165634%401466767085787.

[2] V. Praveen and S. Pillai, "Modeling and simulation of quadcopter using PID controller," *Int. J. Control Theory Appl.*, vol. 9, no. 15, pp. 7151–7158, 2016.

[3] A. Nemati and M. Kumar, "Modeling and control of a single axis tilting quadcopter," in *2014 American Control Conf.*, Portland, OR, USA, Jun. 2014, pp. 3077–3082, doi: 10.1109/ACC.2014.6859328.

[4] A. V. Javir, K. Pawar, S. Dhudum, N. Patale, and S. Patil, "Design, analysis and fabrication of quadcopter," *J. Adv. Res. Mech. Civ. Eng.*, vol. 2, no. 3, pp. 15–23, Mar. 2015, doi: 10.53555/nnmce.v2i3.342.

[5] A. T. Nugraha, "Desain kontrol path following quadcopter dengan algoritma line of sight," in *Pros. SENIATI*, vol. 3, no. 1, Feb. 2017, p. B9. 1–8, doi: 10.36040/seniati.v3i1.1620.

[6] N. Intaratep, W. N. Alexander, W. J. Devenport, S. M. Grace, and A. Dropkin, "Experimental study of quadcopter acoustics and performance at static thrust conditions" in *22nd AIAA/CEAS Aeroacoustics Conf.*, Lyon, France, May 2016, p. 2873, doi: 10.2514/6.2016-2873.

[7] N. Xuan-Mung and S. K. Hong, "Improved altitude control algorithm for quadcopter unmanned aerial vehicles" *Appl. Sci.*, vol. 9, no. 10, p. 2122, May 2019, doi: 10.3390/app9102122.

[8] A. T. Nugraha, "Desain kontrol path following quadcopter dengan command generator tracker model following," M.Si. Thesis, Dept. Elect. Eng., Institut Teknologi Sepuluh Nopember, Surabaya, Indonesia, 2017. [Online]. Available: https://core.ac.uk/download/pdf/291462939.pdf.

[9] U. Seljak and M. Zaldarriaga, "A line of sight approach to cosmic microwave background anisotropies," *Astrophys. J.*, vol. 469, no. 437–444, Mar. 1996, doi: 10.48550/arXiv.astro-ph/9603033.

[10] T. I. Fossen, M. Breivik, and R. Skjetne, "Line-of-sight path following of underactuated marine craft," in *IFAC Proc. Vol.*, vol. 36, no. 21, Sep. 2003, pp. 211–216, doi: 10.1016/S1474-6670(17)37809-6.

[11] W. Zhou *et al.*, "Event-triggered approximate optimal path-following control for unmanned surface vehicles with state constraints," *IEEE Trans. Neural Netw. Learn. Syst.*, pp. 1–15, Jul. 2021, doi: 10.1109/TNNLS.2021.3090054.

[12] W. R. Boswell, J. B. Bingham, and A. J. Colvin, "Aligning employees through "line of sight"," *Bus. Horiz.*, vol. 49, no. 6, pp. 499–509, Dec. 2006, doi: 10.1016/j.bushor.2006.05.001.

[13] A. T. Nugraha, "Disturbance rejection berbasis los saat tracking pada jalur lingkaran menggunakan quadcopter," in *Pros. SENIATI*, vol. 4, no. 1, Feb. 2018, pp. 50–56, doi: 10.36040/seniati.v4i1.313.

[14] W. R. Boswell and J. W. Boudreau, "How leading companies create, measure and achieve strategic results through "line of sight"," *Manag. Decis.*, vol. 39, no. 10, pp. 851–860, Dec. 2001, doi: 10.1108/EUM0000000006525.

[15] K. H. Khalil, "Adaptive output feedback control of nonlinear systems represented by input-output models," *IEEE Trans. Autom. Control*, vol. 41, no. 2, pp. 177–188, Feb. 1996, doi: 10.1109/9.481517.

[16] L. Liu, A. Chen, and Y. J. Liu, "Adaptive fuzzy output-feedback control for switched uncertain nonlinear systems with full-state constraints," *IEEE Trans. Cybern.*, vol. 52, no. 8, Jan. 2021, doi: 10.1109/TCYB.2021.3050510.

[17] A. Levant, "Higher-order sliding modes, differentiation and output-feedback control," *Int. J. Control*, vol. 76, no. 9–10, pp. 924–941, 2003, doi: 10.1080/0020717031000099029.

[18] A. J. Calise, N. Hovakimyan, and M. Idan, "Adaptive output feedback control of nonlinear systems using neural networks," *Automatica*, vol. 37, no. 8, pp. 1201–1211, Aug. 2001, doi: 10.1016/S0005-1098(01)00070-X.

[19] Y. Zhu, N. Xu, X. Chen, and W. X. Zheng, "H∞ control for continuous-time Markov jump nonlinear systems with piecewise-affine approximation," *Automatica*, vol. 141, p. 110300, Jul. 2022, doi: 10.1016/j.automatica.2022.110300.

[20] A. T. Nugraha, I. Anshory, and R. Rahim, "Effect of alpha value change on thrust quadcopter Qball-X4 stability testing using backstepping control," *IOP Conf. Ser.: Mat. Sci. Eng.* vol. 434, no. 1, p. 012207, Nov. 2018, doi: 10.1088/1757-899X/434/1/012207.
[21] A. T. Nugraha, "Design and build a distance and heart rate monitoring system on a dynamic bike integrated with power generating system," *J. Electron., Electromed. Eng., Med. Inf.*, vol. 4, no. 4, pp. 210 – 215, 2022, doi: 10.35882/jeeemi.v4i4.260.